

## Tailoring detection bands of InAs quantum-dot infrared photodetectors using $\text{In}_x\text{Ga}_{1-x}\text{As}$ strain-relieving quantum wells

Eui-Tae Kim, Zhonghui Chen, and Anupam Madhukar<sup>a)</sup>

*Nanostructure Materials and Devices Laboratory, Departments of Materials Science and Physics, University of Southern California, Los Angeles, California 90089-0241*

(Received 25 June 2001; accepted for publication 29 August 2001)

We report on tailoring detection bands of InAs quantum-dot infrared photodetectors (QDIPs) using  $\text{In}_x\text{Ga}_{1-x}\text{As}$  strain-relieving capping layers that also act as quantum wells (QWs). QDIPs with InAs QDs capped by a 20 ML  $\text{In}_{0.15}\text{Ga}_{0.85}\text{As}$  QW show a sharp photoresponse at  $\sim 9 \mu\text{m}$ , while the counterpart QDIPs without QWs show broad photoresponse in the  $5\text{--}7 \mu\text{m}$  range. The excited states involved in the intraband transitions in QDIPs with the  $\text{In}_{0.15}\text{Ga}_{0.85}\text{As}$  QW appear to be coupled QD and QW electron excited states. © 2001 American Institute of Physics.  
[DOI: 10.1063/1.1417513]

Strain-driven coherent island<sup>1</sup> based InAs/GaAs quantum dots (QDs) (Ref. 2) have been studied intensively for applications such as normal-incidence quantum-dot infrared photodetectors (QDIPs) (Refs. 3–8) and lasers.<sup>9–13</sup> For infrared (IR) detector applications, QDIPs have ideally several advantages over quantum-well infrared photodetectors (QWIPs). Compared to QWIPs, QDIPs can have lower dark current and higher photoelectric gain,<sup>14</sup> besides also being intrinsically sensitive to normally incident radiation. Recently, QDIPs based on In(Ga)As/GaAs QDs have been studied.<sup>3–8</sup> However, studies on tailoring the detection bands of QDIPs have been limited to the use of restricted regimes of InGaAs compositions for strained epitaxial island formation while the capping layer remains  $\text{Al}_x\text{Ga}_{1-x}\text{As}$ .<sup>3–8</sup> An alternative promising approach for the tailoring of the QD electronic structure is to modify the layers below and above the nominally binary InAs coherent islands. Replacing GaAs capping layers by  $\text{In}_x\text{Ga}_{1-x}\text{As}$  layers allows partial strain relief and modification of confinement potential to realize longer-wavelength interband transitions in InAs QDs,<sup>15–17</sup> of value for near-IR detector and laser applications. However, the effects of  $\text{In}_x\text{Ga}_{1-x}\text{As}$  barrier layers on intraband transitions in InAs QDs for mid- and long-wavelength IR (LWIR) detectors and lasers have not been reported. In this letter, we report some results of the effect of an  $\text{In}_x\text{Ga}_{1-x}\text{As}$  capping layer on the LWIR photoresponse arising from electron intraband transitions.

We have carried out systematic studies of InAs/ $\text{In}_x\text{Ga}_{1-x}\text{As}$ /GaAs QD structures in the range  $x = 0.1\text{--}0.2$  and thickness of  $5\text{--}60$  ML for the capping layer over InAs islands utilizing photoluminescence (PL), PL excitation (PLE) spectroscopy, and transmission electron microscopy.<sup>18</sup> Guided by these, QDIP structures in the  $n\text{--}i(\text{QD})\text{--}n$  configuration were grown with the objective of realizing the LWIR photoresponse in the important  $8\text{--}12 \mu\text{m}$  window. We find that about 20-ML-thick  $\text{In}_{0.15}\text{Ga}_{0.85}\text{As}$  capping layers on InAs QDs formed for 2.0 ML InAs deposition provide good photoresponse at  $\sim 9 \mu\text{m}$ . Moreover, the  $\text{In}_{0.15}\text{Ga}_{0.85}\text{As}$  layer regions between the InAs QDs are ex-

pected to act as a quantum well (QW) having its own energy states. Tailoring of the thickness, composition, and positioning of the  $\text{In}_x\text{Ga}_{1-x}\text{As}$  capping layers thus allows also tailoring of the position of the QW energy states with respect to the QD bound states. Indeed, in the work reported here, we find that the LWIR photoresponse involves QD intraband transitions to final states that are likely coupled to the QW electron energy states.

The QDIP samples were grown on semi-insulating GaAs(001) substrates via solid-source molecular-beam epitaxy (MBE) under As pressure of  $7 \times 10^6$  Torr. A schematic of the InGaAsQDIP structures is shown in Fig. 1. The QDIP samples consist of an undoped active InAs QD region sandwiched between highly Si-doped GaAs contact layers. First, a Si-doped GaAs contact layer was grown at the growth rate of 0.5 ML/s at  $600^\circ\text{C}$ . Next, a 220-ML-thick undoped GaAs layer was grown at 0.25 ML/s and then an undoped InAs QD layer was formed by 2.0 ML InAs depo-

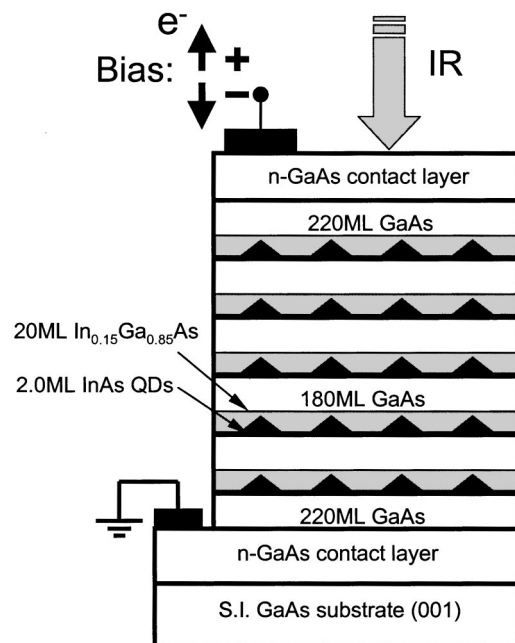


FIG. 1. Schematic of InGaAsQDIP growth and device structure.

<sup>a)</sup>Electronic mail: madhukar@usc.edu

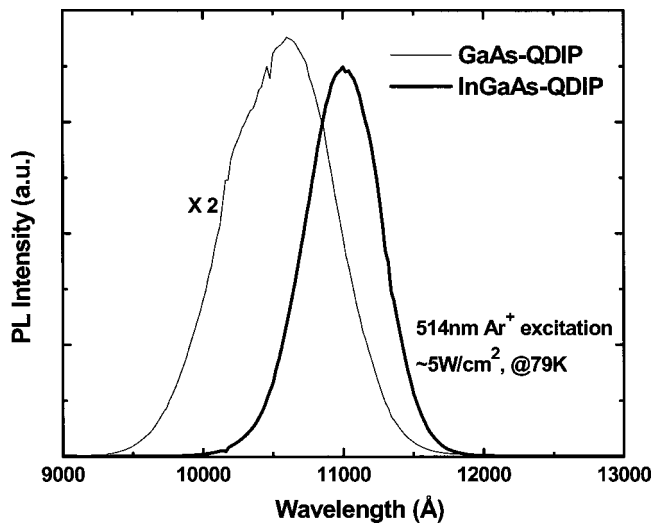


FIG. 2. PL spectra of the GaAs and InGaAs QDIPs at 79 K.

sition at the growth rate of 0.22 ML/s at 500 °C. The InAs QD layer was followed by two types of capping/spacer layers. One type of QDIPs has a 100 ML GaAs capping layer that is also the spacer layer for multilayered QD regions and will be referred to as the GaAs QDIPs. The other type of QDIPs has a 20 ML  $\text{In}_{0.15}\text{Ga}_{0.85}\text{As}$  capping layer followed by 180 ML GaAs as a spacer, referred to here as the InGaAs QDIPs. In both types of structures, the first 40 ML of growth, following InAs QD formation, was via migration-enhanced epitaxy (MEE) at 350 °C to minimize intermixing with the InAs QDs.<sup>19</sup> The rest of the GaAs spacer was grown by conventional MBE growth at 500 °C. These InAs QD layers and spacers were repeated five times and another 220-ML-thick GaAs layer was deposited. Last, a highly Si-doped GaAs contact layer was grown at 500 °C to complete the  $n-i(\text{QD})-n$  configuration suited for electron intraband transition based QDIPs.

For photocurrent measurements, circular mesas of 250  $\mu\text{m}$  diameter were formed using ultraviolet photolithography and wet-chemical etching. As top and bottom Ohmic contacts, AuGe/Ni/Au was e-beam deposited on the highly Si-doped GaAs layers and followed by rapid thermal annealing. In order to characterize intraband transitions of such QDIPs, intraband photocurrent spectroscopy was performed utilizing a Fourier transform infrared (FTIR) spectrometer integrated with a cryostat and a current preamplifier. All photocurrent (PC) data were acquired in the normal-incidence configuration and the bias polarity indicated is relative to the grounded bottom contact.

Figure 2 shows the PL spectra of the GaAs and InGaAs QDIPs at 79 K. The GaAs QDIP has a peak at 1.06  $\mu\text{m}$  with a full width at half maximum (FWHM) of 100 meV. The PL peak position of the InGaAs QDIP is redshifted to 1.10  $\mu\text{m}$  (FWHM of 65 meV) due to a lower potential confinement effect and the strain relaxation effect of the 20 ML  $\text{In}_{0.15}\text{Ga}_{0.85}\text{As}$  cap layer. Normal-incidence FTIR intraband photocurrent spectra of the GaAs and InGaAs QDIPs were measured as a function of bias. Figure 3 shows the behavior at a bias of +0.42 and +0.4 V at 80 K, respectively. The GaAs QDIP has a strong photoresponse over a relatively wide range of 5–7  $\mu\text{m}$ . In that range, there are a few PC

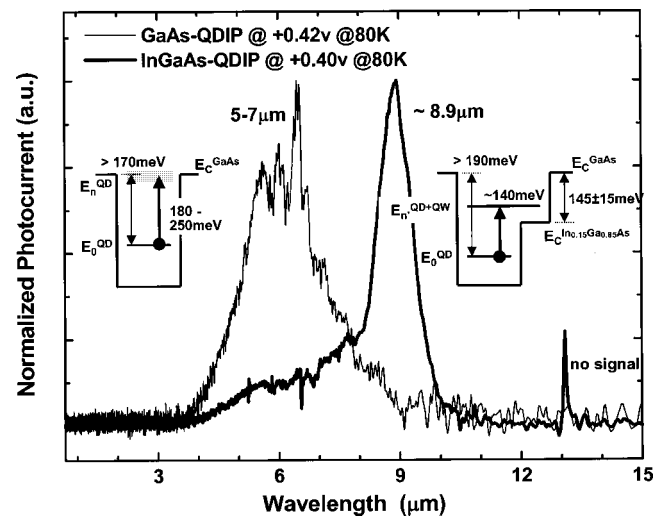


FIG. 3. Intraband photocurrent spectra and schematic energy-band diagrams of GaAs and InGaAs QDIPs at biases of +0.42 and +0.4 V at 80 K, respectively. The equivalent monochromatic optical excitation power is  $\sim 10^{-7}$  W.

peaks rather than a single broad peak. The InGaAs QDIP has a strong sharp peak at  $\sim 9 \mu\text{m}$  with a FWHM of only 16 meV. Figure 4 shows the intraband peak photoresponse of the InGaAs QDIP and the dark currents of the InGaAs and GaAs QDIPs as a function of bias at 80 K. The intraband photoresponse and dark current increase rapidly with increasing bias. In the case of the InGaAs QDIP, above  $\pm 1.2$  V, the photocurrent begins to drop. This is a negative differential photocurrent phenomenon.<sup>3,7,20</sup> Note that the dark current of the InGaAs QDIPs is two to four orders of magnitude smaller than that of the GaAs QDIPs. This is a combined effect of the larger binding energy for the QD electron ground state with respect to the GaAs band edge in the InGaAs QDIP as compared to in the GaAs QDIP and the thicker spacer layers in the former, as noted earlier.

To gain insight into the nature of the electronic states responsible for the observed intraband photoresponse, we have analyzed the above data and a summary is schematically indicated in the band diagrams for the InAs QDs in the GaAs QDIPs and in InGaAs QDIPs shown as insets in Fig.

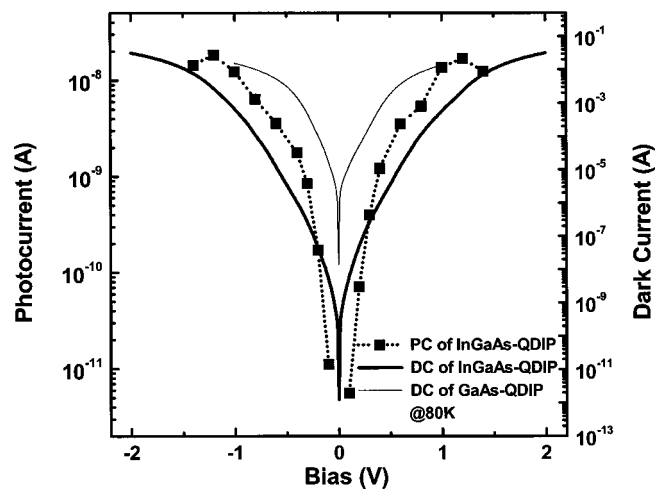


FIG. 4. Photocurrent of the InGaAs QDIP and dark current of the GaAs and InGaAs QDIPs as a function of bias at 80 K.

3. These are drawn for a line passing through the QD base center and apex. Since the stress at the pyramidal island/barrier layer interface is well known to vary with position, note that the true three-dimensional confinement potential is not symmetric in the vertical direction even for GaAs cap layers. For the InGaAs cap layers there is the added contribution of spatially inhomogeneous distribution of In content in the interfacial region. We consider the intraband transitions of both QDIPs to originate from the QD electron ground state since less than two electrons occupy a QD in these QDIP structures.<sup>7</sup> Lower limits on the binding (localization) energies of the QD ground states in the two types of QDIPs can be obtained from the PL peak positions of Fig. 2 as follows. Subtracting the observed PL peak positions of 1.170 eV (1.06  $\mu\text{m}$ ) for the GaAs QDIP and 1.127 eV (1.10  $\mu\text{m}$ ) for the InGaAs QDIP from 1.508 eV (band gap of GaAs at 79 K), we obtain the sum of the binding energies of the ground-state electrons and holes as  $\sim 340$  and  $\sim 380$  meV for the two QDIPs, respectively. Then, using the well-known fact that the binding energy of the electron ground state is significantly higher than that for the hole ground state, we can safely conclude that the electron ground-state binding energies are greater than half of the values noted above for the sum of the electron and hole binding energies, i.e., larger than 170 meV for QDs in the GaAs QDIP and larger than 190 meV for QDs in the InGaAs QDIP. Since the GaAs QDIP has a strong PC response in the range of 5–7  $\mu\text{m}$  (180–250 meV), the electron excited states involved in the intraband transitions in this structure seem to be mainly those located near the GaAs conduction-band edge. By contrast, the intraband PC peak in the InGaAs QDIP is at  $\sim 140$  meV, significantly smaller than the minimum binding energy of  $\sim 190$  meV for the QD electron ground state, and thus indicating that the excited final states involved must be at least 50 meV below the GaAs conduction-band edge. In this case, however, the electron states of the 20-ML-thick  $\text{In}_{0.15}\text{Ga}_{0.85}\text{As}$  cap layer acting as a QW defined by the conduction-band discontinuity between the GaAs and strained  $\text{In}_{0.15}\text{Ga}_{0.85}\text{As}$  conduction bands in the regions between the QDs should be considered. The ratio of the conduction-band discontinuity to the band-gap difference for the  $\text{In}_x\text{Ga}_{1-x}\text{As}/\text{GaAs}$  strained system has been considered to lie in the range of 0.58 (Ref. 21) to 0.70.<sup>22</sup> The conduction-band offset of GaAs and strained  $\text{In}_{0.15}\text{Ga}_{0.85}\text{As}$  ( $\Delta E_c$ ) is then 130–160 meV. Thus, the excited states involved in the intraband transitions are likely located above the conduction-band edge of  $\text{In}_{0.15}\text{Ga}_{0.85}\text{As}$ , as shown in the inset of Fig. 3. In such a situation, the QD electron excited states can be coupled with the  $\text{In}_{0.15}\text{Ga}_{0.85}\text{As}$  QW electron states that lie in the  $\sim 145$  meV region between the GaAs and  $\text{In}_{0.15}\text{Ga}_{0.85}\text{As}$  conduction-band edges. Identifying the origin of the excited states must await appropriate theoretical analysis and we hope these findings provide incentive to our theory colleagues.

In conclusion, we have presented an approach to tailoring the detection bands of QDIPs using  $\text{In}_x\text{Ga}_{1-x}\text{As}$  cap layers as both strain-relieving and QW layers. While the GaAs QDIPs have a strong photoresponse in the 5–7  $\mu\text{m}$  range, InGaAs QDIPs show a strong photoresponse  $\sim 9$   $\mu\text{m}$  with a narrow FWHM of 16 meV. The  $\text{In}_x\text{Ga}_{1-x}\text{As}$  QW electron energy states seem to contribute to the LWIR intraband transitions in the InGaAs QDIPs through coupling with QD electron excited states. These results also indicate one of the ways to exploit a combination of zero-dimensional (QD) and two-dimensional (QW) systems for specific applications.

This work was supported by AFOSR under the MURI98 program on Nanoscience.

- <sup>1</sup>S. Guha, A. Madhukar, and K. C. Rajkumar, Appl. Phys. Lett. **57**, 2110 (1990).
- <sup>2</sup>D. Bimberg, M. Grundmann, and N. Ledentsov, *Quantum Dot Heterostructures* (Wiley, New York, 1998).
- <sup>3</sup>S. J. Xu, S. J. Chua, T. Mei, X. C. Wang, X. H. Zhang, G. Karunasiri, W. J. Fan, C. H. Wang, J. Jiang, S. Wang, and X. G. Xie, Appl. Phys. Lett. **73**, 3153 (1998).
- <sup>4</sup>S. Maimon, E. Finkman, G. Bahir, S. E. Schacham, J. M. Garcia, and P. M. Petroff, Appl. Phys. Lett. **73**, 2003 (1998).
- <sup>5</sup>J. Phillips, P. Bhattacharya, S. W. Kennerly, D. W. Beekman, and M. Dutta, IEEE J. Quantum Electron. **35**, 936 (1999), and references therein.
- <sup>6</sup>E. Towe and D. Pan, IEEE J. Sel. Top. Quantum Electron. **6**, 408 (2000), and references therein.
- <sup>7</sup>Z. H. Chen, O. Baklenov, E. T. Kim, I. Mukhametzhonov, J. Tie, A. Madhukar, Z. Ye, and J. C. Campbell, J. Appl. Phys. **89**, 4558 (2001).
- <sup>8</sup>H. C. Liu, M. Gao, J. McCaffrey, Z. R. Wasilewski, and S. Fafard, Appl. Phys. Lett. **78**, 79 (2001).
- <sup>9</sup>D. Bimberg, N. N. Ledentsov, M. Grundmann, N. Kirstaedter, O. Schmidt, V. M. Ustinov, A. Yu. Egorov, A. E. Zhukov, P. S. Kop'ev, Zh. I. Alferov, S. S. Ruvimov, U. Gösele, and J. Heydenreich, Jpn. J. Appl. Phys., Part 1 **35**, 1311 (1996).
- <sup>10</sup>Q. Xie, A. Kalburge, P. Chen, and A. Madhukar, IEEE Photonics Technol. Lett. **8**, 965 (1996).
- <sup>11</sup>T. Uchida and H. Ischikawa, IEEE Photonics Technol. Lett. **7**, 1385 (1995).
- <sup>12</sup>G. T. Lui, A. Stintz, H. Li, T. C. Newell, A. L. Gray, P. M. Varangis, K. J. Malloy, and L. F. Lester, IEEE J. Quantum Electron. **36**, 1272 (2000).
- <sup>13</sup>G. Park, O. B. Shchekin, and D. G. Deppe, IEEE J. Quantum Electron. **36**, 1065 (2000).
- <sup>14</sup>V. Ryzhii, Semicond. Sci. Technol. **11**, 759 (1996).
- <sup>15</sup>K. Nishi, H. Saito, S. Sugou, and J. S. Lee, Appl. Phys. Lett. **74**, 1111 (1999).
- <sup>16</sup>V. M. Ustinov, N. A. Maleev, A. E. Zhukov, A. R. Kovsh, A. Yu. Egorov, A. V. Lunev, B. V. Volovik, I. L. Krestnikov, Yu. G. Musikhin, N. A. Bert, P. S. Kop'ev, Zh. I. Alferov, N. N. Ledentsov, and D. Bimberg, Appl. Phys. Lett. **74**, 2815 (1999).
- <sup>17</sup>F. Guffarth, R. Heitz, A. Schliwa, O. Steir, A. R. Kovsh, V. Ustinov, N. N. Ledentsov, and D. Bimberg, Phys. Status Solidi B **224**, 61 (2001).
- <sup>18</sup>E. T. Kim, Z. H. Chen, and A. Madhukar (unpublished).
- <sup>19</sup>Q. Xie, P. Chen, A. Kalburge, T. R. Ramachandran, A. Nayfonov, A. Konkar, and A. Madhukar, J. Cryst. Growth **150**, 357 (1995).
- <sup>20</sup>V. Ryzhii, Appl. Phys. Lett. **78**, 3346 (2001).
- <sup>21</sup>D. J. Arent, K. Deneffe, C. Van Hoof, J. De Boeck, and G. Borghs, J. Appl. Phys. **66**, 1739 (1989).
- <sup>22</sup>G. Ji, D. Huang, U. K. Reddy, T. S. Henderson, R. Houdré, and H. Morkoç, J. Appl. Phys. **62**, 3366 (1987).